Cell

Malaria Parasite *clag3* Genes Determine Channel-Mediated Nutrient Uptake by Infected Red Blood Cells

Wang Nguitragool,[1,4] Abdullah A.B. Bokhari,[1,4] Ajay D. Pillai,[1,4] Kempaiah Rayavara,[1] Paresh Sharma,[1] Brad Turpin,[2] L. Aravind,[3] and Sanjay A. Desai[1,*]

[1]The Laboratory of Malaria and Vector Research, National Institute of Allergy and Infectious Diseases, National Institutes of Health, Rockville, MD 20852, USA

[2]National Instruments, Inc., Austin, TX 78730, USA

[3]National Center for Biotechnology Information, National Library of Medicine, National Institutes of Health, Bethesda, MD 20892, USA

[4]These authors contributed equally to this work

*Correspondence: sdesai@niaid.nih.gov

DOI 10.1016/j.cell.2011.05.002

SUMMARY

Development of malaria parasites within vertebrate erythrocytes requires nutrient uptake at the host cell membrane. The plasmodial surface anion channel (PSAC) mediates this transport and is an antimalarial target, but its molecular basis is unknown. We report a parasite gene family responsible for PSAC activity. We used high-throughput screening for nutrient uptake inhibitors to identify a compound highly specific for channels from the Dd2 line of the human pathogen *P. falciparum*. Inheritance of this compound's affinity in a Dd2 × HB3 genetic cross maps to a single parasite locus on chromosome 3. DNA transfection and in vitro selections indicate that PSAC-inhibitor interactions are encoded by two *clag3* genes previously assumed to function in cytoadherence. These genes are conserved in plasmodia, exhibit expression switching, and encode an integral protein on the host membrane, as predicted by functional studies. This protein increases host cell permeability to diverse solutes.

INTRODUCTION

Successful intracellular development of malaria parasites depends on directed remodeling of the host erythrocyte cytosol and plasma membrane. For example, *P. falciparum* and all studied malaria parasites increase erythrocyte permeability to numerous solutes including nutrients required for intracellular parasite growth. Sugars, amino acids, purines, vitamins, and the cation choline are needed for in vitro propagation and have increased permeability after infection (Homewood and Neame, 1974; Ginsburg et al., 1985; Upston and Gero, 1995; Saliba et al., 1998; Staines et al., 2000). Anions and antimalarial toxins also have increased uptake (Kirk et al., 1994; Hill et al., 2007; Lisk et al., 2008). Intriguingly, the parasite nevertheless maintains a low Na^+ permeability at the host membrane to avoid osmotic lysis in the bloodstream (Cohn et al., 2003).

New antimalarial drugs are desperately needed. Conservation of erythrocyte permeability changes in divergent malaria parasites suggests that the responsible mechanism may be a suitable drug target (Lisk and Desai, 2005). Interest has been further increased by the recognition that the parasite can alter the permeability to acquire resistance to antimalarials (Hill et al., 2007; Lisk et al., 2008).

Despite its central role in parasite biology and therapeutic potential, the origin and precise nature of the uptake mechanism have been controversial. Electrophysiological studies over the past decade have implicated transmembrane transport through one or more ion channels on the erythrocyte surface (Desai et al., 2000; Staines et al., 2007). Although there is agreement that these channels are anion selective and that they appear on the host membrane some hours after parasite invasion, the genes responsible for each proposed ion channel remain unknown. Some studies have proposed activation of quiescent human channels intrinsic to the erythrocyte (Decherf et al., 2004; Duranton et al., 2004; Verloo et al., 2004), whereas others support one or more parasite-encoded proteins trafficked to the host membrane. The plasmodial surface anion channel (PSAC) is the primary candidate for a parasite-encoded ion channel (Alkhalil et al., 2004), but computational analyses of completed parasite genomes have not revealed orthologs of classical anion channels.

We have now used a genetic approach to identify a parasite gene family involved in PSAC activity. Our studies combine high-throughput screens for novel channel inhibitors, electrophysiology revealing direct action on PSAC, linkage analysis in a *P. falciparum* genetic cross, DNA transfection experiments, in-vitro selections, and mutant analysis to demonstrate the role of two paralogous genes in PSAC activity. We propose that these genes contribute to a novel microbial ion channel for the uptake of diverse nutrient solutes.

RESULTS

High-Throughput Screen Identifies Isolate-Specific Inhibitors

We searched for small-molecule inhibitors with differing efficacies against channels induced by divergent parasite lines. Such

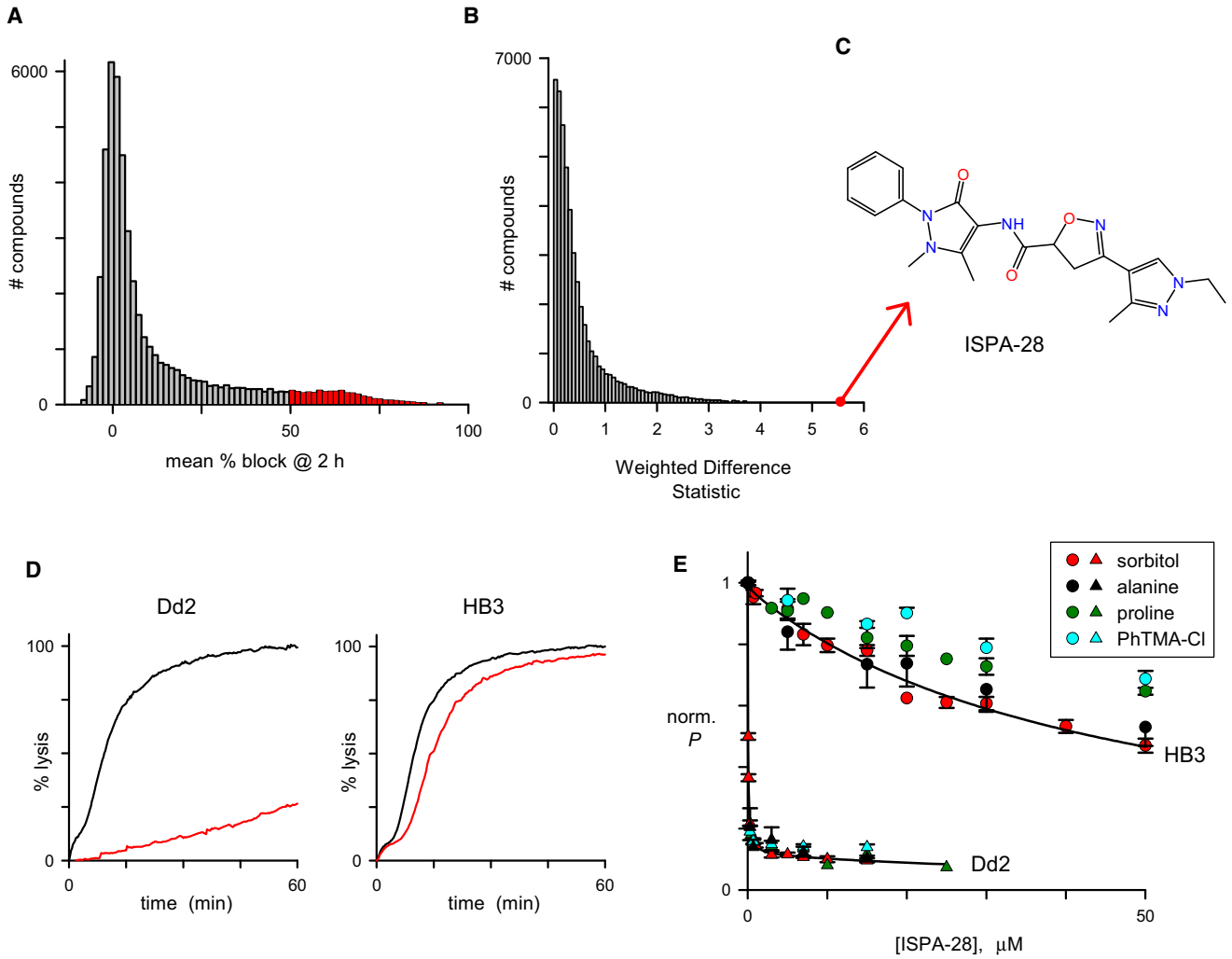

Figure 1. High-Throughput Screen and a Dd2-Specific Inhibitor

(A) All-points histogram of mean % block at 2 hr for 48,157 compounds screened against sorbitol uptake by red blood cells infected with HB3 or Dd2 lines, calculated according to Equation 2. Red shading reflects compounds having % block ≥50, corresponding to inhibitory $K_{0.5}$ values ≤1 μM (Pillai et al., 2010).

(B) All-points histogram of the normalized statistic WDS for these compounds (Equation 3). Most compounds have WDS <1.0, indicating negligible difference in activity against channels on HB3 and Dd2.

(C) Structure of ISPA-28, a Dd2-specific inhibitor (WDS = 5.6; see also Figure S1).

(D) Continuous recordings of osmotic lysis kinetics in sorbitol for indicated parasites without or with 7 μM ISPA-28 (black and red traces, respectively).

(E) Dose responses for inhibition of organic solute permeability (*P*) into HB3- and Dd2-infected cells (circles and triangles, respectively). Symbols represent the mean ± standard error of the mean (SEM) of up to eight measurements each. Solid lines represent best fits to Equation 1.

inhibitors presumably bind to one or more variable sites on the channel, which may result either from polymorphisms in a parasite channel gene or from differing activation of human channels. To find these inhibitors, we used a transmittance-based assay that tracks osmotic lysis of infected cells in sorbitol, a sugar alcohol with increased permeability after infection (Wagner et al., 2003). This assay has previously been adapted to 384-well format and used to find high-affinity PSAC inhibitors (Pillai et al., 2010). Here, we used this format to screen a library of compounds against erythrocytes infected with the HB3 and Dd2 *P. falciparum* lines. To maximize detection of hits, we chose a low stringency in our screens by using library compounds at a high concentration (10 μM) and by reading each microplate at multiple time points (Pillai et al., 2010). Figure 1A tallies the all-points histogram for compound activity averaged from screens of both lines. Eight percent of compounds met or exceeded the threshold of 50% normalized block at 2 hr (Equation 2), consistent with a low screening stringency. We then defined a weighted difference statistic (WDS, Equation 3) that normalizes measured differences in efficacy against HB3 and Dd2 channels to the standard deviation of positive control wells in each microplate. An all-points histogram of this parameter revealed that 86% of all compounds produced indistinguishable effects on the two parasite lines (WDS ≤ 1.0, Figure 1B). Thus, most inhibitor-binding sites are conserved.

Nevertheless, a small number of compounds produced significantly differing activities in the two screens. One such inhibitor, named ISPA-28 (for isolate-specific PSAC antagonist based on studies described below, Figure 1C), was reproducibly more effective at inhibiting sorbitol uptake by Dd2- than by HB3-infected cells. Secondary studies with ISPA-28 revealed an ~800-fold difference in half-maximal affinities (Figures 1D and 1E) ($K_{0.5}$ values of 56 ± 5 nM versus 43 ± 2 μM for Dd2 and HB3, respectively; $p < 10^{-10}$).

We also examined ISPA-28 effects on uptake of the amino acids alanine and proline as well as the organic cation phenyltrimethylammonium (PhTMA), solutes with known increases in permeability after infection (Ginsburg et al., 1985; Bokhari et al., 2008). Each solute's permeability was inhibited with dose responses matching those for sorbitol (Figure 1E), providing strong evidence for a single shared transport mechanism used by these diverse solutes.

We next tested 22 different laboratory parasite lines and found significant transport inhibition with only Dd2 and W2 (Figure S1 available online). Because Dd2 was generated by prolonged drug selections starting with W2 (Wellems et al., 1988), their channels' distinctive ISPA-28 affinities suggest a stable heritable element in the parasite genome.

ISPA-28 Interacts Directly with PSAC

To explore the mechanism of ISPA-28 block, we performed patch-clamp of infected erythrocytes. Using the whole-cell configuration, we observed similar currents on HB3- and Dd2-infected cells in experiments without known inhibitors (Figures 2A and 2B). These currents exhibited inward rectification. Previous studies have determined that they are carried primarily by anions with a permeability rank order of $SCN^- > I^- > Br^- > Cl^-$ (Desai et al., 2000). ISPA-28 reduced their magnitudes but had a significantly greater effect on Dd2-infected cells ($p < 10^{-9}$, n = 22–28 cells each). In the cell-attached configuration with 1.1 M Cl^- as the charge carrier, ion channel activity characteristic of PSAC was detected on both lines (~20 pS slope conductance with fast flickering gating) (Alkhalil et al., 2004); without inhibitor, channels from the two lines were indistinguishable (Figure 2C). However, recordings with 10 μM ISPA-28 revealed a marked difference as Dd2 channels were near-fully inhibited whereas HB3 channels were largely unaffected (Figures 2D and 2F) (n = 6–7 channel molecules each; $p < 0.0002$). Thus, this compound's effects on single PSAC recordings parallel those on uptake of sorbitol and other organic solutes.

We analyzed closed durations from extended recordings and determined that ISPA-28 imposes a distinct population of long block events, but only in recordings on Dd2-infected cells (Figure S2). At the same time, intrinsic channel closings, which occur in the absence of inhibitor, were conserved on both parasites and were not affected by ISPA-28 (events of < 20 ms duration in Figure S2).

Inheritance of ISPA-28 Efficacy in a Dd2 × HB3 Genetic Cross

We next examined ISPA-28 efficacy against PSAC activity on red blood cells infected with recombinant progeny clones from the Dd2 × HB3 genetic cross (Wellems et al., 1990). For each clone, we examined sorbitol uptake in the absence and presence of 7 μM ISPA-28, a concentration that optimally distinguishes the parental channel phenotypes, and quantified inhibition (Equation 2). Although a few of the 34 independent progeny clones exhibited intermediate channel inhibition, most resembled one or the other parent (Figure 3A). Quantitative trait locus (QTL) analysis was used to search for associations between ISPA-28 efficacy and inheritance of available microsatellite markers. A primary scan identified a single significant peak having a logarithm of odds (LOD) score of 12.6 at the proximal end of chromosome 3 (Figure 3B). A secondary scan for residual effects did not find additional peaks reaching statistical significance (Figure S3).

The mapped locus contains 42 predicted genes (Table S1). Although none have homology to classical ion channels from other organisms, many are conserved in other plasmodia, as expected for the responsible gene(s) from conservation of PSAC activity in malaria parasites (Lisk and Desai, 2005). The mapped region is enriched in genes encoding proteins destined for export to host cytosol ($p < 10^{-4}$ by simulation), as typical of apicomplexan subtelomeric regions. Some of the encoded proteins have one or more predicted transmembrane domains as usually involved in channel pore formation, but this criterion may miss some transport proteins. The PEXEL motif, which directs parasite proteins to the host cell (Marti et al., 2004), was present in some genes, but this module is not universally required for export (Spielmann and Gilberger, 2010). Thus, computational analyses suggested several candidates but could not specifically implicate any as ion channel components.

piggyBac-Mediated Complementations Implicate Two Genes

We therefore selected a DNA transfection approach and chose *piggyBac* transposase to complement Dd2 parasites with the HB3 allele of individual candidate genes (Balu et al., 2005). This method has the disadvantage that successfully transfected parasites will carry both parental alleles and therefore be merodiploid for candidate genes. Nevertheless, we reasoned that the marked difference in ISPA-28 efficacy between the parental lines should produce a detectable change in transport phenotype upon complementation with the responsible gene. Importantly, the high efficiency of random integration conferred by *piggyBac* permits rapid examination of many genes (Balu et al., 2009).

We cloned 14 genes with their endogenous 5′ and 3′ untranslated regions (UTRs) from the HB3 parent into the pXL-BacII-DHFR plasmid; a 15th construct containing a conserved but not annotated open reading frame (ORF 147 kb) was also prepared. Each was transfected individually along with a helper plasmid encoding the transposase into Dd2 parasites (Figure 4A). Selection for hDHFR expression yielded parasites that stably carry both Dd2 and HB3 alleles for each candidate. Because an altered channel phenotype presumably requires expression of the HB3 allele, we used reverse transcriptase PCR to amplify polymorphic regions of each gene and sequenced the amplicons to determine whether both parental alleles were transcribed; this approach confirmed expression of 12 candidates (Figure 4B, asterisks). We then performed ISPA-28 dose responses for inhibition of sorbitol uptake by erythrocytes infected with each transfectant (Figures 4B and 4C). Two transfectants, expressing HB3

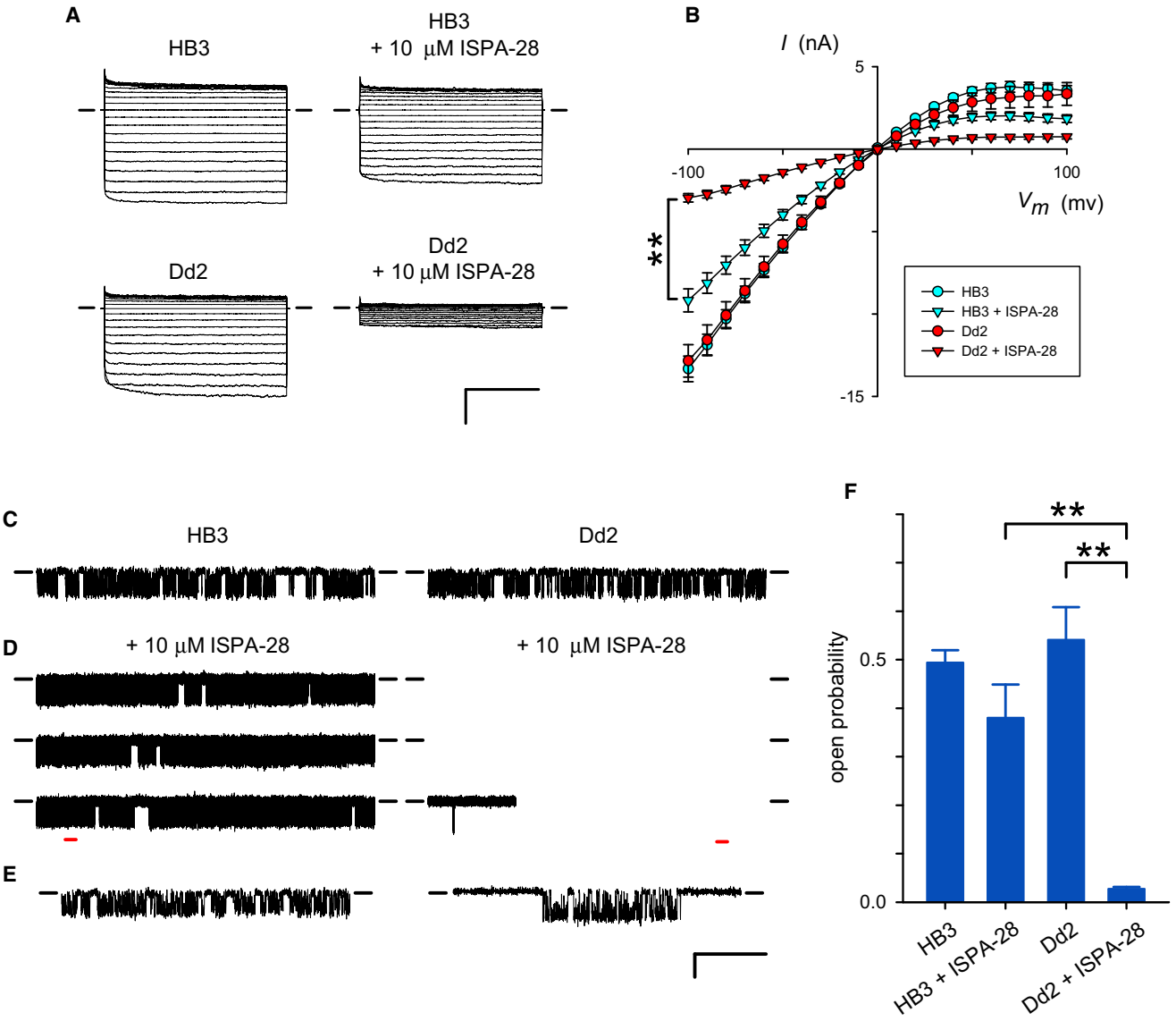

Figure 2. ISPA-28 Interacts Directly with PSAC to Block Transport

(A) Whole-cell patch-clamp recordings on erythrocytes infected with indicated parasite lines without or with addition of 10 μM ISPA-28 to bath and pipette solutions. Ensemble traces represent responses to pulses of −100 to +100 mV (10 mV increments). Horizontal and vertical scale bars represent 20 ms and 5 nA, respectively.

(B) Current-voltage relationships showing mean ± SEM whole-cell currents determined from up to 28 cells each. **$p < 10^{-9}$.

(C) Single PSAC recordings on HB3- or Dd2-infected erythrocytes without inhibitor (left and right columns, respectively).

(D) Single-channel recordings from these lines with 10 μM ISPA-28 in bath and pipette solutions.

(E) Resolved intrinsic gating in the presence of ISPA-28, expanded from the bottom traces in (D) as indicated with red dashes. Black dashes adjacent to each trace represent the closed channel level. Horizontal scale bar = 100 ms, 2 s, or 74 ms (panels C, D, and E, respectively); vertical scale bar = 3 pA for all panels. All whole-cell and cell-attached recordings used symmetric bath and pipette solutions of 1 M choline chloride, 115 mM NaCl, 10 mM $MgCl_2$, 5 mM $CaCl_2$, 20 mM Na-HEPES (pH 7.4).

(F) Mean ± SEM single-channel open probability for indicated lines in the absence or presence of 10 μM ISPA-28. **$p < 0.0002$.

See also Figure S2.

alleles for PFC0110w and PFC0120w, produced significant changes in ISPA-28 efficacy with $K_{0.5}$ values between those of Dd2 and HB3, as expected for cells carrying channels from both parental lines ($p = 0.01$ and $p < 10^{-7}$ in comparison to Dd2, respectively). Limiting dilution cloning of the PFC0120w transfectant yielded a clone, Dd2-*pB*120w, that had undergone at least one integration event (Figure S4); its ISPA-28 $K_{0.5}$ was indistinguishable from the transfection pool (not shown). For both genes, quantitative analyses suggest relatively low-level expression of the HB3 allele because the transfectant $K_{0.5}$ values

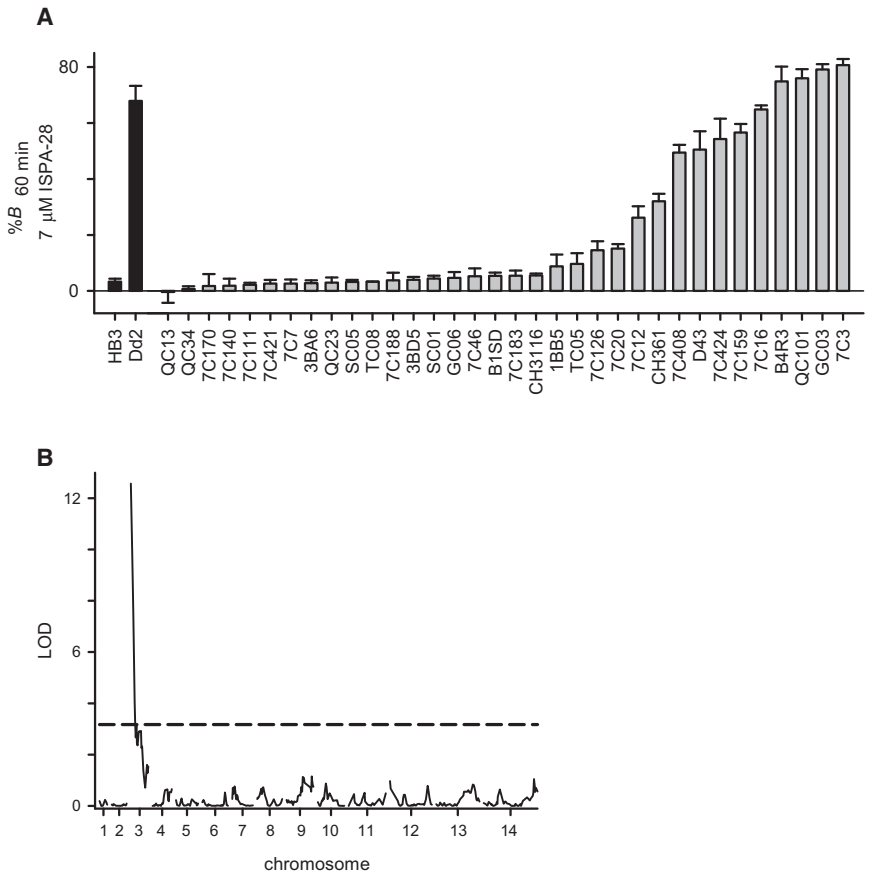

Figure 3. Inheritance of ISPA-28 Affinity in a Genetic Cross and QTL Analysis

(A) Mean ± SEM block of sorbitol uptake by 7 μM ISPA-28 for indicated parental lines and progeny clones at a 60 min time point according to Equation 2.

(B) Logarithm of odds (LOD) scores from a primary scan of QTL associated with ISPA-28 efficacy. The peak (LOD of 12.6) maps to the 5′ end of chromosome 3. Dashed line is the 0.05 significance threshold calculated from 1000 permutations.

See also Figure S3.

(95 ± 8 and 140 ± 12 nM) are closer to those of Dd2 than of HB3. Expression levels of the two parental alleles may be influenced by the genomic environment of the integration site, relative promoter efficiencies, and a gene-silencing mechanism examined below.

Allelic Exchange Confirms a Role for These Genes

PFC0120w and PFC0110w are members of the *clag* multigene family conserved in *P. falciparum* and all examined plasmodia; the family's name is based on proposed roles as *c*ytoadherence-*l*inked *a*nti*g*ens. These paralogs are known as *clag3.1* and *clag3.2*, respectively, based on their locations on chromosome 3; *P. falciparum* carries three additional paralogs on chromosomes 2, 8, and 9.

To examine the unexpected possibility that *clag3* products contribute to PSAC activity, we used an allelic exchange strategy designed to transfer potent ISPA-28 block from the Dd2 line to HB3 parasites. Because Dd2 parasites express *clag3.1* but not *clag3.2* (Kaneko et al., 2005; see also next section), their *clag3.1* gene presumably encodes high ISPA-28 affinity. We therefore constructed a transfection plasmid carrying a 3.2 kb fragment from the 3′ end of the Dd2 *clag3.1* allele, an in-frame C-terminal FLAG tag followed by a stop codon, and the fragment gene's 3′ UTR (pHD22Y-120w-flag-PG1, Figure 5A). Because this plasmid carries only a gene fragment and lacks a leader sequence to drive expression, an altered transport phenotype requires recombination into the parasite genome. We transfected HB3 with this plasmid and used PCR to screen for integration into each of the five endogenous *clag* genes. This approach detected recombination into the HB3 *clag3.2* gene; limiting dilution cloning yielded HB3^{3rec}, a clone carrying a single site integration event without residual episomal plasmid (Figures S5A and S5B). DNA sequencing indicated recombination between single-nucleotide polymorphisms at 3718 and 4011 bp from the HB3 *clag3.2* start codon. This recombination site corresponds to successful transfer of downstream polymorphisms including a recognized hypervariable region at 4266–4415 bp; contamination with other laboratory parasite lines was excluded by fingerprinting (Figure S5C).

PSAC activity on HB3^{3rec} exhibited a marked increase in ISPA-28 efficacy (Figure 5B), further supporting a role for *clag3* genes in sorbitol and nutrient uptake. Although this allelic exchange strategy yielded a gene replacement in contrast to the complementations achieved with *piggyBac*, the channel's ISPA-28 affinity was again intermediate between those of HB3 and Dd2 (Figure 5C). Several mechanisms may contribute to the quantitatively incomplete transfer of inhibitor affinity. First, two or more polymorphic sites on the protein might contribute to ISPA-28 binding. If some of these sites are upstream from the recombination event, the resulting chimeric protein may have functional properties distinct from those of either parental line. Second, the channel may contain additional unidentified subunits; here, transfection to replace each contributing HB3 gene with Dd2 alleles might be required to match the ISPA-28 affinity of Dd2. Finally, in addition to the chimeric *clag3.2*$_{HB3}$-*3.1*$_{Dd2}$ gene produced by transfection, HB3^{3rec} also carries the *clag3.1* gene endogenous to HB3 parasites. Expression of both paralogs could also produce an intermediate ISPA-28 affinity.

To explore these possibilities, we performed cell-attached patch-clamp on HB3^{3rec}-infected cells. Individual channel molecules exhibiting ISPA-28 potencies matching those of each parental line were identified (Figures S5D–S5F). These

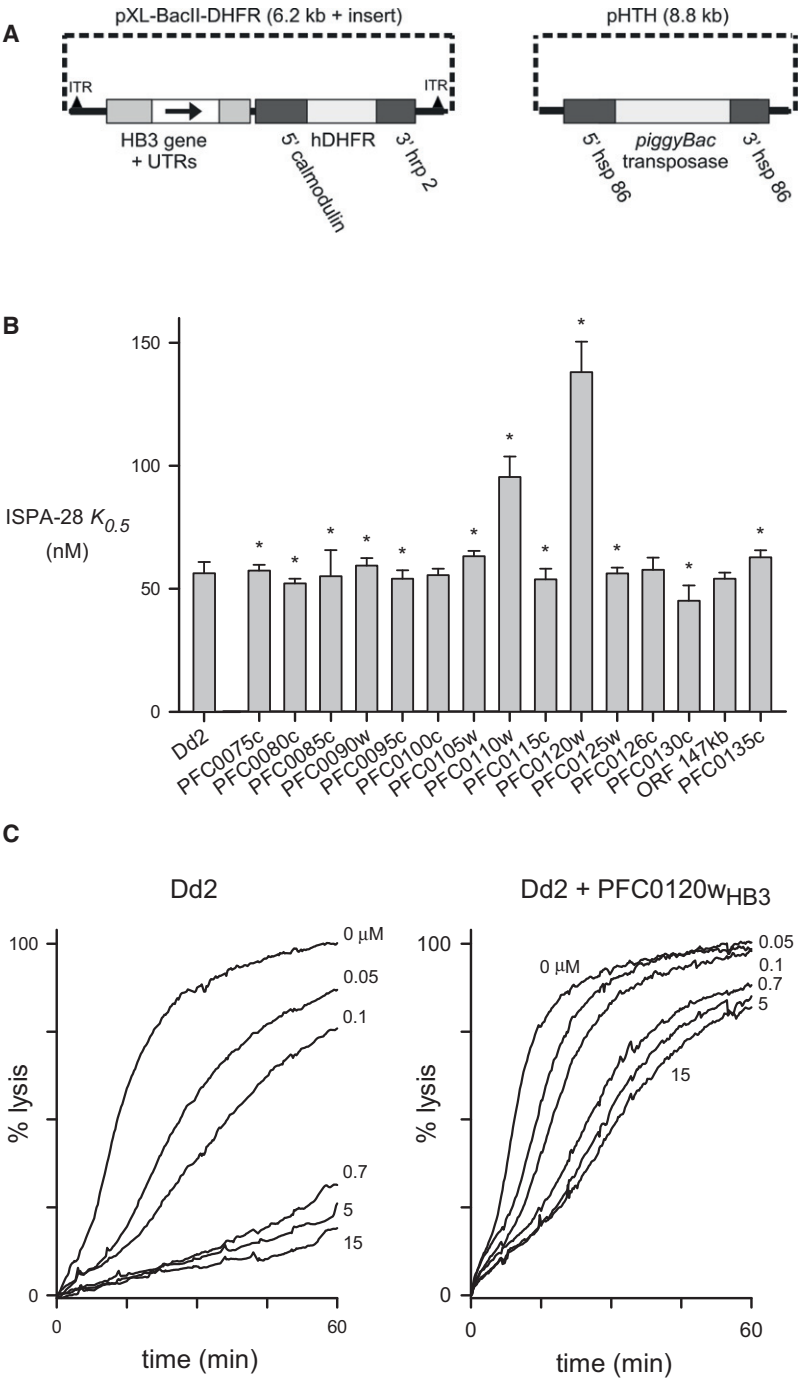

Figure 4. Complementation Implicates Two *clag* Genes

(A) Schematic shows the plasmid maps for the translocon vector into which genes from the HB3 line were cloned (left) and the helper plasmid (right). See also Figure S4 and Table S2.

(B) Mean ± SEM. ISPA-28 $K_{0.5}$ values for Dd2 without or after complementation with the indicated genes from HB3. * indicates confirmed expression of the HB3 allele in the transfectant.

(C) Osmotic lysis kinetics showing significant decrease in ISPA-28 efficacy after transfection with PFC0120w. [ISPA-28] in micromolar as indicated.

recordings exclude scenarios that require a homogenous population of channels with intermediate ISPA-28 affinity but are consistent with several other mechanisms.

clag3 Gene Silencing and Switched Expression Determine Inhibitor Affinity

In addition to the complex behavior of HB3^{3rec}, we noticed that certain progeny from the genetic cross had lower ISPA-28 affinity than Dd2 despite inheriting the mapped chromosome 3 locus fully from the Dd2 parent (notably 7C20, 7C12, and CH361 in Figure 3A and dose responses in Figure 6A). Because subtelomeric multigene families in *P. falciparum* are susceptible to recombination and frequent gene conversion events (Freitas-Junior et al., 2000), we sequenced both *clag3* paralogs and neighboring genomic DNA from 7C20 and Dd2 but did not find DNA-level differences. We therefore considered epigenetic mechanisms that may influence ISPA-28 affinity. *clag3.1* and *clag3.2* have been reported to undergo mutually exclusive expression (Cortés et al., 2007). Monoallelic expression and switching, also documented for other gene families in *P. falciparum* (Chen et al., 1998; Lavazec et al., 2007), allow individual parasites to express a single member of a multigene family. Daughter parasites resulting from asexual reproduction continue exclusive expression of the same gene through incompletely understood epigenetic mechanisms (Howitt et al., 2009). After a few generations, some daughters may switch to expression of another member of the gene family, affording diversity that contributes to immune evasion (Scherf et al., 2008).

We performed reverse transcriptase PCR and found that Dd2 expresses *clag3.1* almost exclusively whereas the three discordant progeny express *clag3.2* at measurable levels (Figure 6B), suggesting epigenetic regulation. We therefore applied selective pressure to progeny cultures with osmotic lysis in sorbitol solutions containing ISPA-28. Inclusion of ISPA-28 preferentially spares infected cells whose channels have high inhibitor affinity: these cells incur less sorbitol uptake and do not lyse (Figure 1D). These selections, applied on multiple consecutive days, yielded marked reductions in parasitemia. Surviving parasites exhibited improved ISPA-28 affinity quantitatively matching that of the Dd2 parent (Figure 6C). Identical selections applied to HB3 and three progeny inheriting its chromosome 3 locus did not change

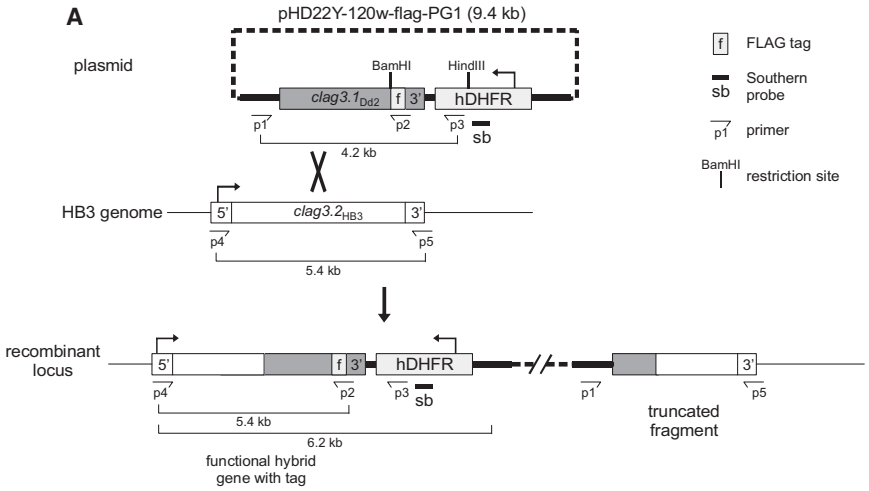

Figure 5. Allelic Exchange Yields an Intermediate Phenotype

(A) Schematic shows the integration plasmid (top) and the result of single homologous recombination between the plasmid's Dd2 *clag3.1* fragment and genomic *clag3.2* of HB3. See primer sequences in Table S3.

(B) Sorbitol-induced osmotic lysis kinetics for the allelic exchange clone HB3^{3rec} with indicated [ISPA-28].

(C) Mean ± SEM ISPA-28 dose response for HB3^{3rec} (circles). This dose response is intermediate between those of HB3 and Dd2 (top and bottom solid lines, respectively; taken from fits in Figure 1E).

See also Figure S5.

ISPA-28 affinity (Figure 6D, n = 3–4 separate attempts each; data for progeny clones QC13, SC01, and 7C421 not shown), excluding effects of the selections on unrelated genomic sites.

Real-time qPCR using primers specific for each of the 5 *clag* genes revealed that selection with sorbitol and ISPA-28 reproducibly increased *clag3.1* expression while decreasing that of *clag3.2* in progeny inheriting the Dd2 locus (Figure 6E; expression ratios in Figure 6F). Selections applied to the parental HB3 line were without effect (Figure 6F), consistent with its unchanged inhibitor affinity. Although these selections did not alter relative expression of other paralogs (*clag2*, *clag8*, and *clag9*), we cannot exclude their possible contributions to PSAC activity.

Selections were also applied to HB3^{3rec}, which carries a chimeric *clag3.2*$_{HB3}$-*3.1*$_{Dd2}$ transgene and the *clag3.1* gene native to HB3. In contrast to the lack of effect on the isogenic HB3 line, these synchronizations increased the transfectant's ISPA-28 affinity to a $K_{0.5}$ of 51 ± 9 nM, matching that of Dd2 channels (Figures 6D and 6G). This change in channel phenotype correlated with a near exclusive expression of the transgene (Figure 6H, first time point), confirming that expression of HB3 *clag3.1* by a subset of cells accounts for the intermediate ISPA-28 affinity observed in Figure 5E. These findings also delimit the determinants of ISPA-28 binding to polymorphic sites within the Dd2 *clag3.1* gene fragment transferred to HB3^{3rec}.

Expression switching in *P. falciparum* multigene families occurs over several generations and should lead to a drift in population phenotype. After selection of the chimeric gene in HB3^{3rec}, continued in vitro propagation yielded a gradual decay in ISPA-28 affinity that correlated with decreasing transgene expression (Figures 6G and 6H). As with other multigene families (Lavazec et al., 2007), several factors may affect the steady-state ISPA-28 affinity and relative expression levels for the two *clag3* genes upon continued culture without selective pressure.

Reverse Selections with a Distinct ISPA

We next sought a PSAC inhibitor with reversed specificity for the two Dd2 *clag3* products. To this end, we surveyed hits from our high-throughput screen using the progeny clone 7C20 before and after selection for *clag3.1* expression. This secondary screen identified ISPA-43 as a PSAC inhibitor with an allele specificity opposite that of ISPA-28 (Figure 6I and Figure S6B, $K_{0.5}$ of 32 and 3.9 µM for channels associated with *clag3.1* and *clag3.2* genes from Dd2, respectively). We then applied sorbitol synchronizations with 4 µM ISPA-43 to the *clag3.1*-expressing 7C20 culture and achieved robust reverse selection: the surviving parasites exhibited both low ISPA-28 affinity and a reversed *clag3* expression profile (Figures 6J and 6K). Thus, inhibitors can be used in purifying selections of either *clag3* gene. Because ISPA-28 affinity can be reduced either through drift without selective pressure or by selection for the alternate paralog with an inhibitor having reversed

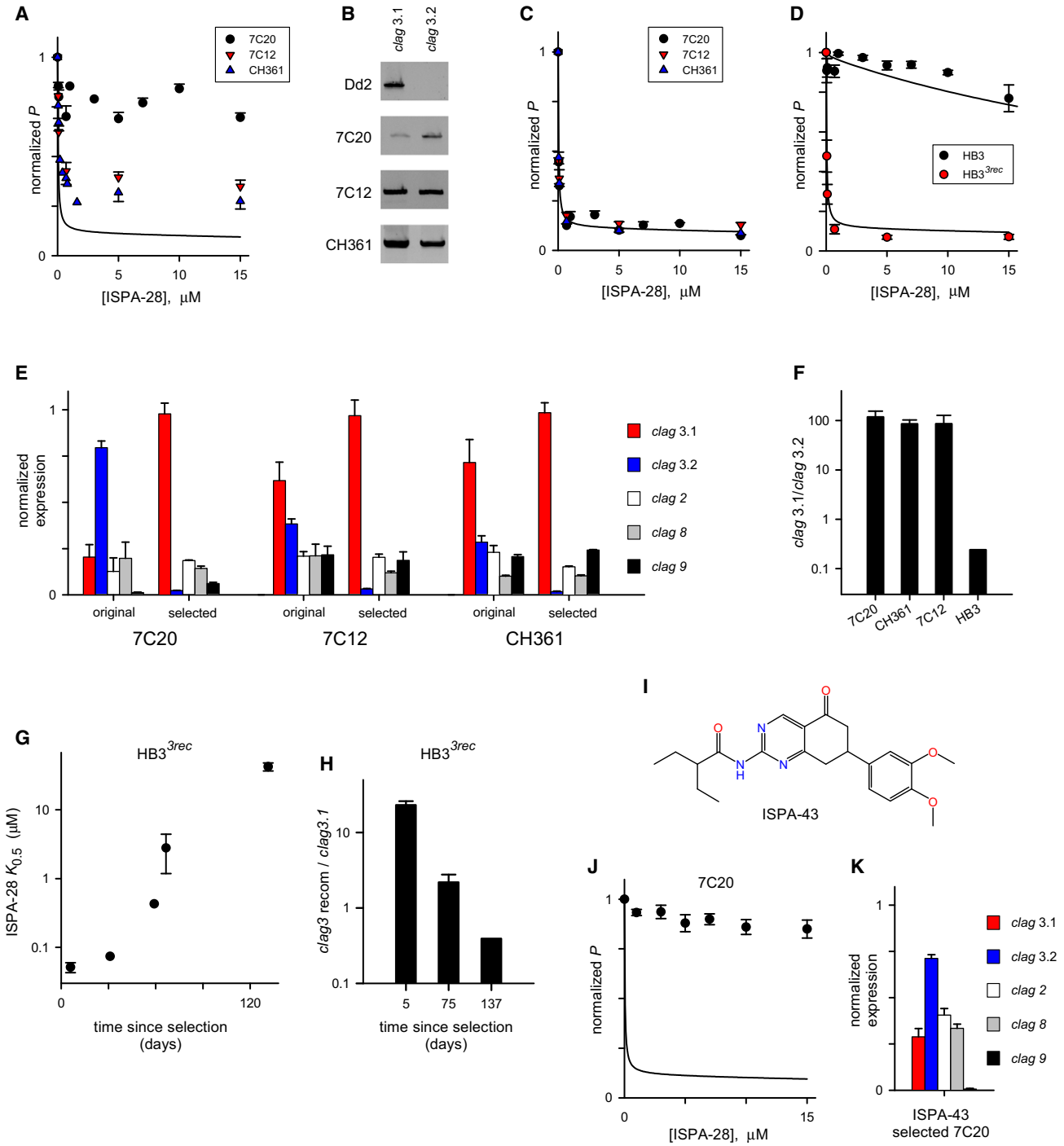

Figure 6. Relative Expression of *clag3* Alleles Determines ISPA-28 Affinity

(A) Mean ± SEM ISPA-28 dose responses for indicated progeny (symbols) and the expected efficacy based on inheritance of the locus from Dd2 (solid line).

(B) Ethidium-stained gels showing relative expression of *clag3* alleles in indicated lines. Amplicons represent full-length cDNA.

(C and D) Transport inhibition dose responses after in vitro selections with sorbitol and ISPA-28. Selection does not change HB3′s dose response but improves that of HB3^{3rec} and indicated progeny to levels matching Dd2′s. Symbols represent mean ± SEM for indicated lines; solid lines represent parental phenotypes from Figure 1E.

(E) Expression patterns for *clag* genes in indicated lines before and after in vitro selection, determined by quantitative RT-PCR. Mean ± SEM of replicates; see also Table S4.

(F) *clag3.1*:*clag3.2* expression ratio after selections of indicated lines, showing that lines isogenic with Dd2 at the *clag3* locus are strongly purified, whereas HB3 is not. Mean ± SEM values calculated from up to four RNA harvests each.

specificity, these studies mitigate concerns about indirect effects of exposure to sorbitol or individual inhibitors.

clag3 Mutation in a Leupeptin-Resistant PSAC Mutant

A stable parasite mutant with altered PSAC selectivity, gating, and pharmacology was recently generated by in vitro selection of HB3 with leupeptin (Lisk et al., 2008). We sequenced *clag3* genes from this mutant, HB3-*leuR1*, and identified a point mutation within its *clag3.2* gene that changes the conserved A1210 to a threonine (Figure 7A and Figure S7A), consistent with a central role of *clag3* genes in solute uptake. HB3-*leuR1* silences its unmodified *clag3.1* and preferentially expresses the mutated *clag3.2* (expression ratio of 19.2 ± 1.5, determined as in Figure 6F), as required for a direct effect on PSAC behavior. This mutation is within a predicted transmembrane domain and may directly account for the observed changes in channel gating and selectivity. Because HB3-*leuR1* may carry additional genome-level changes, further studies will be needed to determine the precise role of the A1210T mutation in leupeptin resistance.

clag3 Products Are Exposed at the Host Erythrocyte Surface

To directly contribute to PSAC activity, at least some of the *clag3* product must associate with the host membrane, presumably as an integral membrane protein. We therefore raised polyclonal antibodies to a carboxy-terminal recombinant fragment conserved between the two *clag3* products. Confocal microscopy with this antibody confirmed reports localizing these proteins to the host cytosol and possibly the erythrocyte membrane as well as within rhoptries of invasive merozoites (Vincensini et al., 2008) (Figure S7B). To obtain more conclusive evidence, we used immunoblotting to examine susceptibility of these proteins to extracellular protease. Without protease treatment, a single ~160 kDa band was detected in whole-cell lysates, consistent with the expected size of *clag3* products (Figure 7B). Treatment with pronase E under conditions designed to prevent digestion of intracellular proteins reduced the amount of the full-length protein and revealed a 35 kDa hydrolysis fragment. In contrast, a monoclonal antibody against KAHRP, a parasite protein that interacts with the host membrane cytoskeleton but is not exposed (Kilejian et al., 1991), confirmed that intracellular proteins are resistant to hydrolysis under our conditions (Figure 7C). As reported for another protease (Baumeister et al., 2006), pronase E treatment significantly reduced PSAC-mediated sorbitol uptake (Figure 7D); this effect was sensitive to protease inhibitors, suggesting that proteolysis at one or more exposed sites interferes with transport.

Ultracentrifugation of infected cell lysates revealed that the *clag3* product is fully membrane associated (Figure 7E); a fraction could, however, be liberated by treatment with Na_2CO_3, which strips membranes of peripheral proteins (Fujiki et al., 1982). Because this fraction was protease insensitive, it reflects an intracellular pool of *clag3* product loosely associated with membranes. The C-terminal hydrolysis fragment was present only in the carbonate-resistant insoluble fraction, indicating an integral membrane protein.

Because our polyclonal antibodies might cross-react with *clag* products from other chromosomes, we next examined protease sensitivity in HB3^{3rec}, whose chimeric *clag3* transgene encodes a C-terminal FLAG tag. Anti-FLAG antibody recognized a single integral membrane protein in HB3^{3rec} and no proteins from the parental HB3 line, indicating specificity for the recombinant gene product (Figure 7F). Treatment with pronase E prior to cell lysis and fractionation revealed a hydrolysis fragment indistinguishable from that seen with the antibody raised against the native protein's C terminus.

DISCUSSION

We have used high-throughput screening to identify ISPA-28, an inhibitor with remarkable specificity for solute uptake by erythrocytes infected with Dd2 parasites. Patch-clamp studies revealed that this compound acts specifically on PSAC. Because its activity is restricted to one parasite lineage (Figure S1), ISPA-28 addresses previous concerns regarding inhibitor specificity and implicates a central role for PSAC in anion and nutrient transport at the host membrane. We then tracked inheritance of ISPA-28 efficacy in the Dd2 × HB3 genetic cross and identified a single parasite genomic locus. Gene complementation, allelic exchange, in vitro selections using ISPA-28, and a point mutation in a known PSAC mutant implicate two *clag* genes from this locus.

A transport role for members of the *clag* gene family is unexpected because the encoded proteins already have proposed roles unrelated to transport. The first *clag* gene was identified via a chromosome 9 deletion event linked to loss of infected erythrocyte binding to melanoma cells (Schmidt et al., 1982; Day et al., 1993). *clag9* is present in the deletion locus and appears to function in infected cell cytoadherence to the endothelial receptor CD36 (Trenholme et al., 2000). Other *clag* genes, identified through the *P. falciparum* genome sequencing project, were presumed to serve related functions. Proposals have included infected cell binding to various endothelial receptors (Holt et al., 1999), merozoite invasion of erythrocytes (Rungruang et al., 2005; Kaneko, 2007), or as a chaperone for protein export (Craig, 2000; Vincensini et al., 2008; Goel et al., 2010). The role for *clag3* products in solute transport requires a broader view for functions of this gene family; this role is compatible with two previous observations. First, isolated disruption of *clag9*

(G) Kinetics of decrease in ISPA-28 efficacy for HB3^{3rec} upon continuous in vitro culture after end of ISPA-28 selection. Mean ± SEM from up to five trials each.
(H) Kinetics of decreasing expression of the chimeric *clag3.2*$_{HB3}$-*3.1*$_{Dd2}$ transgene in HB3^{3rec} after cessation of ISPA-28 selection, presented as mean ± SEM of the expression ratio relative to the endogenous *clag3.1*.
(I) Structure of ISPA-43. See also Figure S6.
(J) Reversed selection using ISPA-43. 7C20 culture previously selected for *clag3.1* using ISPA-28 (panel C) was subjected to sorbitol synchronizations in the presence of ISPA-43. Graphic shows ISPA-28 dose response (circles, mean ± SEM) and that of the parental Dd2 (solid line).
(K) qRT-PCR expression profile for 7C20 after reversed selection using ISPA-43. Mean ± SEM of replicates.

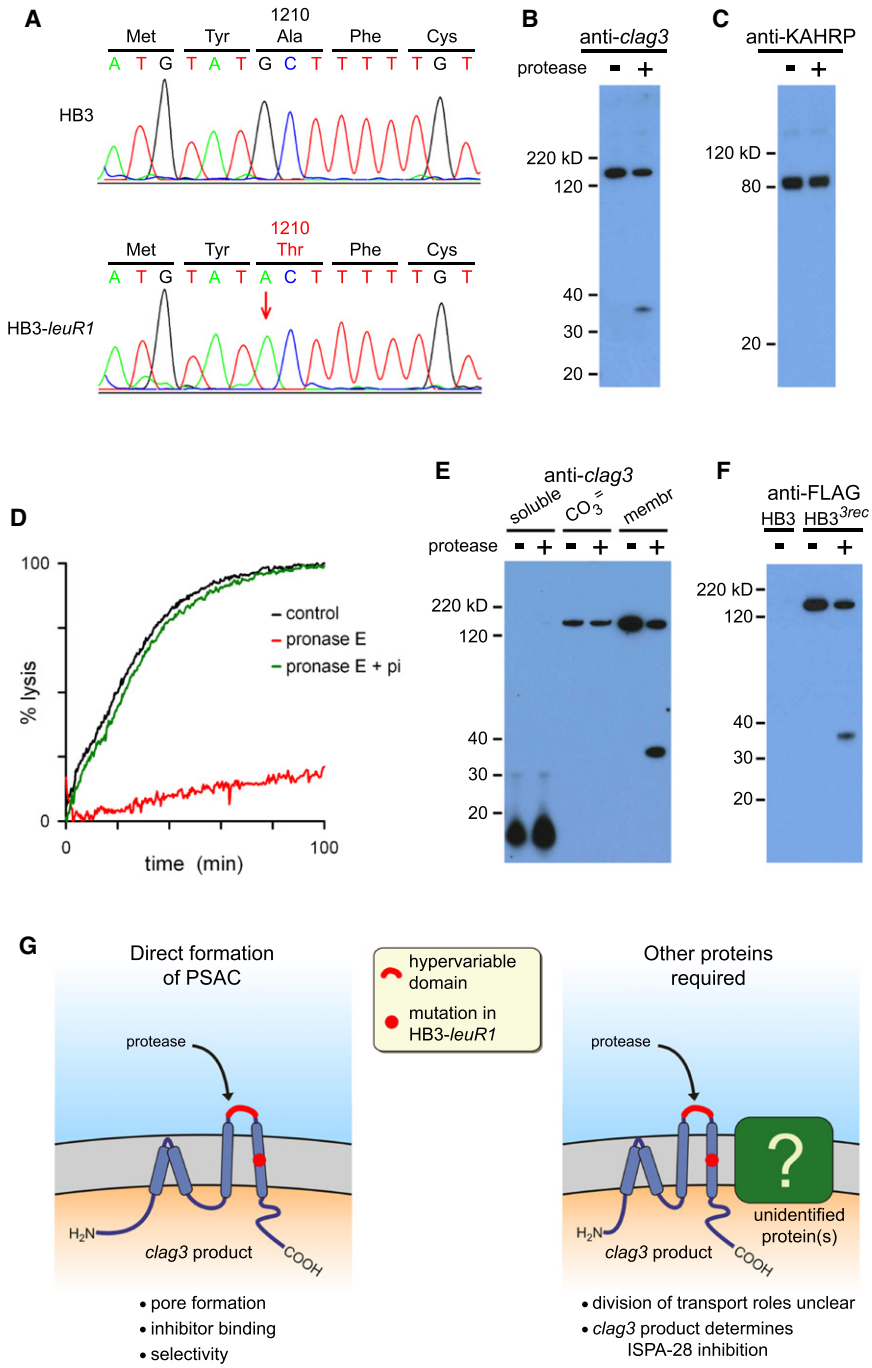

Figure 7. *clag3* Mutant Analysis and Host Membrane Localization

(A) Sequence chromatograms from wild-type HB3 and mutant HB3-*leuR1* showing the point mutation (red arrow) that changes A1210 to threonine.

(B) Immunoblot of total lysate from HB3-infected cells without or with protease treatment of intact cells. Blot was probed with a polyclonal antibody to a recombinant *clag3* fragment.

(C) Control immunoblot showing that the intracellular parasite protein KAHRP is not hydrolyzed by protease treatment.

(D) Osmotic lysis kinetics without or with protease treatment, showing that PSAC activity is degraded by pronase E. Addition of protease inhibitors prevents loss of channel activity (pronase E + pi, green trace).

(E) Immunoblot showing that the protein is membrane associated and partially extractable with carbonate treatment ($CO_3^=$), and that the protease hydrolysis fragment is an integral membrane protein (membr).

(F) Immunoblot of carbonate-extracted membranes from HB3 and HB3^{3rec} without or with protease treatment as indicated. Blot was probed with anti-FLAG tag antibody, which does not recognize HB3 and is specific for the recombinant *clag3* product.

(G) Schematic shows two models for the role of the *clag3* product in PSAC formation. A pronase E cleavage site, a known hypervariable domain, and the site of the HB3-*leuR1* mutation are indicated. Our studies support an intracellular C terminus; the transmembrane topology shown is speculative and based on computational analysis. The green box (right panel) represents additional parasite or host protein(s) that may contribute to channel activity.

See also Figure S7.

abolishes melanoma cell binding (Trenholme et al., 2000), suggesting that other *clag* products cannot compensate for loss of that member. Second, mutually exclusive expression of *clag3.1* and *clag3.2* despite constitutive expression of other family members has been reported (Cortés et al., 2007), suggesting that *clag3* products may serve roles requiring greater protection from immune challenge. Our transport-based in vitro selections confirm this atypical gene regulation: whereas purifying selection for one or the other *clag3* genes was readily achieved, significant changes in expression of other members were not detected (Figure 6).

The encoded proteins share a conserved α-helical CLAG domain also present in RON2, a rhoptry neck protein implicated in erythrocyte invasion (Richard et al., 2010; Anantharaman et al., 2007). Whereas *clag* genes are present only in plasmodia, RON2 is more widely distributed in apicomplexan parasites and appears to be the ancestral member (Figure S6A). Phylogenetic analysis suggests that after divergence from RON2, *clag* genes underwent expansion and split into two distinct groups early in the *Plasmodium* lineage. One group, typified by *clag9* in *P. falciparum*, contains a single member in each plasmodium, whereas the second group has from one to four members in each species. Interestingly, both RON2 and the *clag* products are packaged into rhoptries, organelles present in the extraerythrocytic merozoite (Kaneko et al.,

2001); they are then secreted into the host cell upon invasion (Ling et al., 2004; Vincensini et al., 2008).

Recognizing that *clag3* encodes an integral protein at the host erythrocyte membrane, we envision two models for how the protein may contribute to channel activity. In one, the *clag3* product alone forms a novel microbial nutrient and ion channel (Figure 7G, left diagram). In the other, the *clag3* product interacts with one or more other proteins to form functional PSAC (Figure 7G, right diagram). Multisubunit channels are well established with individual components contributing to solute recognition and permeation, channel gating, inhibitor or ligand binding, and/or other regulatory functions. If there are additional subunits, they might be either parasite-encoded or resident host proteins; the identities of the additional proteins as well as the roles served by each would need to be determined.

Several findings are relevant to the discussion of these models. First, *clag* genes are present in all plasmodial species but absent from other apicomplexan genera, paralleling transport studies that show PSAC activity in only plasmodia (Alkhalil et al., 2007). Second, a role for *clag3* product in pore formation is suggested by the A1210T mutation in a leupeptin-resistant channel mutant: point mutations in other ion channel genes often yield altered gating and selectivity. Third, the extracellular loop 35 kDa from the protein's C terminus, identified through protease susceptibility studies, exhibits marked variability between *P. falciparum* lines, presumably due to positive selection by host immunity (Figure S6C) (Iriko et al., 2008). Because the Dd2 *clag3.1* gene carries a unique sequence here, this site may define the ISPA-28 binding pocket. Although conventional membrane-spanning regions are missing, the Phobius algorithm detects two conserved hydrophobic segments with high probability of forming transmembrane domains (residues 1000–1062 and residues 1208–1231 in the *clag3.1* product, Figure S7C). These atypical transmembrane domains along with the lack of homology to known ion channels may contribute to PSAC's unusual selectivity and conductance properties, as established by functional studies (Ginsburg and Stein, 1988; Cohn et al., 2003; Bokhari et al., 2008).

Our findings open several new directions for future research. Most importantly, they permit molecular studies into the mechanisms of PSAC-inhibitor interaction and the process of solute recognition and permeation through this unusual channel. A second direction will be to explore the trafficking of parasite-encoded channel components to the host membrane. Surprisingly, the *clag* products are synthesized many hours before channel activity is detectable. As described above, these proteins are packaged into rhoptries, secreted into the host erythrocyte upon invasion, and trafficked across the parasitophorous vacuolar membrane prior to reaching the host membrane. Why is this circuitous route taken when there is a more direct mechanism involving synthesis in the intracellular parasite and signal sequence-mediated export (Boddey et al., 2010; Russo et al., 2010)?

By providing a definitive protein target, our study will also stimulate drug and vaccine development against PSAC (Pillai et al., 2010). Should enthusiasm be tempered by the presence of two paralogous genes, selection for diversity at exposed sites, and variable inhibitor affinities for parasite isolates? While polymorphic sites on the channel have permitted linkage analysis and gene identification, most of the coding region is highly conserved in *P. falciparum* and other malaria parasites, consistent with conserved selectivity and transport biophysics in all infected cells (Lisk and Desai, 2005). Because most inhibitors do not appear to interact with polymorphic sites, targeting critical conserved parts of the protein for drug development will be facilitated by the high-throughput screening approaches used here.

EXPERIMENTAL PROCEDURES

Osmotic Lysis Experiments and High-Throughput Inhibitor Screen

Infected cell osmotic lysis in permeant solutes was used to quantify solute permeabilities and was performed as described (Wagner et al., 2003). Trophozoite stage *P. falciparum* cultures were enriched using the Percoll-sorbitol method, washed, and resuspended at 25°C and 0.15% hematocrit in 280 mM sorbitol, 20 mM Na-HEPES, 0.1 mg/ml BSA (pH 7.4) with inhibitor as indicated; uptake of proline, alanine, or phenyl-trimethylammonium chloride (PhTMA-Cl) was similarly measured after iso-osmotic replacement for sorbitol. Osmotic swelling and lysis were continuously tracked by recording transmittance of 700 nm light through the cell suspension (DU640 spectrophotometer with Peltier temperature control, Beckman Coulter). Recordings were normalized to 100% osmotic lysis at the transmittance plateau. Inhibitor dose responses were calculated by interpolation of the time required to reach fractional lysis thresholds. Dose responses were fitted to the sum of two Langmuir isotherms:

$$P = a/(1 + (x/b)) + (1 - a)/(1 + (x/c)) \quad (1)$$

where P represents the normalized solute permeability in the presence of inhibitor at concentration x, and a, b, and c are constants.

High-throughput inhibitor screens using this transmittance assay were performed as described (Pillai et al., 2010). Screens were performed identically with HB3- and Dd2-infected cells at room temperature using a 50,000 compound library with >90% purity confirmed by NMR (ChemDiv). Individual microplate wells contained single compounds at a 10 μM final concentration. Each microplate also contained two types of controls. Thirty-two positive control wells received PBS instead of sorbitol; erythrocytes in these wells do not lyse because PSAC has low Na^+ permeability. Thirty-two negative control wells received sorbitol with DMSO but no test compound. Readings were taken at multiple time points to permit estimation of inhibitor affinity in a high-throughput format. The purity and molecular weight of ISPA-28 were confirmed by mass spectrometry.

The activity of each screening compound was calculated from readings at the 2 hr time point, according to:

$$\%B = 100 * (A_{cpd} - \bar{A}_{neg}) / (\bar{A}_{pos} - \bar{A}_{neg}) \quad (2)$$

where $\%B$ is the normalized channel block and A_{cpd} represents the absorbance from a test compound well. $\bar{A}_{neg}$ and $\bar{A}_{pos}$ represent the mean absorbances of in-plate negative and positive control wells. $\%B$ is a quantitative measure of inhibitor activity.

Inhibitors having significantly differing efficacies against uptake by HB3- and Dd2-infected cells were selected using a weighted difference statistic (WDS), determined from $\%B$ values at the 2 hr time point according to:

$$WDS = |\%B_{HB3} - \%B_{Dd2}| / (3 * \sigma_{pos}) \quad (3)$$

where σ_{pos} is the standard deviation of in-plate positive control wells. Isolate-specific inhibitors have WDS $\geq$ 1.0; larger values correspond to greater differences in efficacy against uptake by the two screened parasite lines. Analysis and data mining of the screens were automated using locally developed code (DIAdem 10.2 and DataFinder, National Instruments).

Electrophysiology

Whole-cell and single-channel currents were recorded under voltage-clamp conditions using previously described patch-clamp methods (Alkhalil et al., 2004). Details are provided in the Extended Experimental Procedures.

Linkage Analysis to Map Inheritance of ISPA-28 Efficacy

We selected a distinct collection of 443 polymorphic microsatellite markers that distinguish the Dd2 and HB3 parental lines. Five additional single-nucleotide polymorphisms within the chromosome 3 locus were identified by DNA sequencing and were used to genotype progeny clones. These genotype data were used to search for single and interacting genetic loci associated with ISPA-28 efficacy in the cross-progeny by performing QTL analysis with R/qtl software as described (Broman et al., 2003; http://www.rqtl.org/). Because *P. falciparum* asexual stages are haploid, the analysis was analogous to that for recombinant inbred crosses. Significance thresholds at the $p = 0.05$ level were determined by permutation analysis. A secondary scan to search for additional QTL was carried out by controlling for the primary chromosome 3 locus as described in the R/qtl software package.

DNA Transfection of Malaria Parasites

All plasmids were confirmed by restriction digestion and sequencing, propagated in *E. coli* strain XL-10 gold (Strategene), and prepared with EndoFree Plasmid Mega Kit (QIAGEN). Percoll-enriched trophozoites were mixed with plasmid-loaded erythrocytes and allowed to grow for two cycles before application of 5 nM WR99210. Transformed cells were typically detected by microscopic examination within 3–8 weeks. Details are provided in the Extended Experimental Procedures.

SUPPLEMENTAL INFORMATION

Supplemental Information includes Extended Experimental Procedures, seven figures, and four tables and can be found with this article online at doi:10.1016/j.cell.2011.04.022.

ACKNOWLEDGMENTS

We thank John Adams, Alan Cowman, and Thomas Wellems for providing reagents; Mehreen Baakza, Kent Barbian, Yasmin El-Sayed, Juraj Kabat, Glenn Nardone, Son Nguyen, Norton Peet, Steve Porcella, Jose Riberio, Latha Souvannaseng, Kurt Wollenberg, and Albert Youn for technical help; and the NIAID Scientific Director's office for providing required temporary laboratory space. We thank Edwin McCleskey and Thomas Wellems for critical reading of the manuscript. S.D. is a named inventor on a provisional patent application describing the PSAC antimalarial target identified in this article. B.T. is an employee and shareholder of National Instruments, Inc., which markets data analysis software used in this study. This research was supported by the Medicines for Malaria Venture (MMV) and the Intramural Research Program of the National Institutes of Health, National Institute of Allergy and Infectious Diseases, and the National Library of Medicine.

Received: December 24, 2010
Revised: March 21, 2011
Accepted: May 2, 2011
Published: May 26, 2011

REFERENCES

Alkhalil, A., Cohn, J.V., Wagner, M.A., Cabrera, J.S., Rajapandi, T., and Desai, S.A. (2004). *Plasmodium falciparum* likely encodes the principal anion channel on infected human erythrocytes. Blood *104*, 4279–4286.

Alkhalil, A., Hill, D.A., and Desai, S.A. (2007). Babesia and plasmodia increase host erythrocyte permeability through distinct mechanisms. Cell. Microbiol. *9*, 851–860.

Anantharaman, V., Iyer, L.M., Balaji, S., and Aravind, L. (2007). Adhesion molecules and other secreted host-interaction determinants in Apicomplexa: insights from comparative genomics. Int. Rev. Cytol. *262*, 1–74.

Balu, B., Shoue, D.A., Fraser, M.J., Jr., and Adams, J.H. (2005). High-efficiency transformation of *Plasmodium falciparum* by the lepidopteran transposable element *piggyBac*. Proc. Natl. Acad. Sci. USA *102*, 16391–16396.

Balu, B., Chauhan, C., Maher, S.P., Shoue, D.A., Kissinger, J.C., Fraser, M.J., Jr., and Adams, J.H. (2009). *piggyBac* is an effective tool for functional analysis of the *Plasmodium falciparum* genome. BMC Microbiol. *9*, 83.

Baumeister, S., Winterberg, M., Duranton, C., Huber, S.M., Lang, F., Kirk, K., and Lingelbach, K. (2006). Evidence for the involvement of *Plasmodium falciparum* proteins in the formation of new permeability pathways in the erythrocyte membrane. Mol. Microbiol. *60*, 493–504.

Boddey, J.A., Hodder, A.N., Günther, S., Gilson, P.R., Patsiouras, H., Kapp, E.A., Pearce, J.A., de Koning-Ward, T.F., Simpson, R.J., Crabb, B.S., and Cowman, A.F. (2010). An aspartyl protease directs malaria effector proteins to the host cell. Nature *463*, 627–631.

Bokhari, A.A., Solomon, T., and Desai, S.A. (2008). Two distinct mechanisms of transport through the plasmodial surface anion channel. J. Membr. Biol. *226*, 27–34.

Broman, K.W., Wu, H., Sen, S., and Churchill, G.A. (2003). R/qtl: QTL mapping in experimental crosses. Bioinformatics *19*, 889–890.

Chen, Q., Fernandez, V., Sundström, A., Schlichtherle, M., Datta, S., Hagblom, P., and Wahlgren, M. (1998). Developmental selection of var gene expression in *Plasmodium falciparum*. Nature *394*, 392–395.

Cohn, J.V., Alkhalil, A., Wagner, M.A., Rajapandi, T., and Desai, S.A. (2003). Extracellular lysines on the plasmodial surface anion channel involved in Na^+ exclusion. Mol. Biochem. Parasitol. *132*, 27–34.

Cortés, A., Carret, C., Kaneko, O., Yim Lim, B.Y., Ivens, A., and Holder, A.A. (2007). Epigenetic silencing of *Plasmodium falciparum* genes linked to erythrocyte invasion. PLoS Pathog. *3*, e107.

Craig, A. (2000). Malaria: a new gene family (*clag*) involved in adhesion. Parasitol. Today (Regul. Ed.) *16*, 366–367, discussion 405.

Day, K.P., Karamalis, F., Thompson, J., Barnes, D.A., Peterson, C., Brown, H., Brown, G.V., and Kemp, D.J. (1993). Genes necessary for expression of a virulence determinant and for transmission of *Plasmodium falciparum* are located on a 0.3-megabase region of chromosome 9. Proc. Natl. Acad. Sci. USA *90*, 8292–8296.

Decherf, G., Egée, S., Staines, H.M., Ellory, J.C., and Thomas, S.L. (2004). Anionic channels in malaria-infected human red blood cells. Blood Cells Mol. Dis. *32*, 366–371.

Desai, S.A., Bezrukov, S.M., and Zimmerberg, J. (2000). A voltage-dependent channel involved in nutrient uptake by red blood cells infected with the malaria parasite. Nature *406*, 1001–1005.

Duranton, C., Huber, S.M., Tanneur, V., Brand, V.B., Akkaya, C., Shumilina, E.V., Sandu, C.D., and Lang, F. (2004). Organic osmolyte permeabilities of the malaria-induced anion conductances in human erythrocytes. J. Gen. Physiol. *123*, 417–426.

Freitas-Junior, L.H., Bottius, E., Pirrit, L.A., Deitsch, K.W., Scheidig, C., Guinet, F., Nehrbass, U., Wellems, T.E., and Scherf, A. (2000). Frequent ectopic recombination of virulence factor genes in telomeric chromosome clusters of *P. falciparum*. Nature *407*, 1018–1022.

Fujiki, Y., Hubbard, A.L., Fowler, S., and Lazarow, P.B. (1982). Isolation of intracellular membranes by means of sodium carbonate treatment: application to endoplasmic reticulum. J. Cell Biol. *93*, 97–102.

Ginsburg, H., and Stein, W.D. (1988). Biophysical analysis of a novel transport pathway induced in red blood cell membranes by the malaria parasite. Prog. Clin. Biol. Res. *252*, 317–322.

Ginsburg, H., Kutner, S., Krugliak, M., and Cabantchik, Z.I. (1985). Characterization of permeation pathways appearing in the host membrane of *Plasmodium falciparum* infected red blood cells. Mol. Biochem. Parasitol. *14*, 313–322.

Goel, S., Valiyaveettil, M., Achur, R.N., Goyal, A., Mattei, D., Salanti, A., Trenholme, K.R., Gardiner, D.L., and Gowda, D.C. (2010). Dual stage synthesis and crucial role of cytoadherence-linked asexual gene 9 in the surface expression of malaria parasite var proteins. Proc. Natl. Acad. Sci. USA *107*, 16643–16648.

Hill, D.A., Pillai, A.D., Nawaz, F., Hayton, K., Doan, L., Lisk, G., and Desai, S.A. (2007). A blasticidin S-resistant *Plasmodium falciparum* mutant with a defective plasmodial surface anion channel. Proc. Natl. Acad. Sci. USA *104*, 1063–1068.

Holt, D.C., Gardiner, D.L., Thomas, E.A., Mayo, M., Bourke, P.F., Sutherland, C.J., Carter, R., Myers, G., Kemp, D.J., and Trenholme, K.R. (1999). The cytoadherence linked asexual gene family of *Plasmodium falciparum*: are there roles other than cytoadherence? Int. J. Parasitol. *29*, 939–944.

Homewood, C.A., and Neame, K.D. (1974). Malaria and the permeability of the host erythrocyte. Nature *252*, 718–719.

Howitt, C.A., Wilinski, D., Llinás, M., Templeton, T.J., Dzikowski, R., and Deitsch, K.W. (2009). Clonally variant gene families in *Plasmodium falciparum* share a common activation factor. Mol. Microbiol. *73*, 1171–1185.

Iriko, H., Kaneko, O., Otsuki, H., Tsuboi, T., Su, X.Z., Tanabe, K., and Torii, M. (2008). Diversity and evolution of the rhoph1/clag multigene family of *Plasmodium falciparum*. Mol. Biochem. Parasitol. *158*, 11–21.

Kaneko, O. (2007). Erythrocyte invasion: vocabulary and grammar of the *Plasmodium* rhoptry. Parasitol. Int. *56*, 255–262.

Kaneko, O., Tsuboi, T., Ling, I.T., Howell, S., Shirano, M., Tachibana, M., Cao, Y.M., Holder, A.A., and Torii, M. (2001). The high molecular mass rhoptry protein, RhopH1, is encoded by members of the *clag* multigene family in *Plasmodium falciparum* and *Plasmodium yoelii*. Mol. Biochem. Parasitol. *118*, 223–231.

Kaneko, O., Yim Lim, B.Y., Iriko, H., Ling, I.T., Otsuki, H., Grainger, M., Tsuboi, T., Adams, J.H., Mattei, D., Holder, A.A., and Torii, M. (2005). Apical expression of three RhopH1/Clag proteins as components of the *Plasmodium falciparum* RhopH complex. Mol. Biochem. Parasitol. *143*, 20–28.

Kilejian, A., Rashid, M.A., Aikawa, M., Aji, T., and Yang, Y.F. (1991). Selective association of a fragment of the knob protein with spectrin, actin and the red cell membrane. Mol. Biochem. Parasitol. *44*, 175–181.

Kirk, K., Horner, H.A., Elford, B.C., Ellory, J.C., and Newbold, C.I. (1994). Transport of diverse substrates into malaria-infected erythrocytes via a pathway showing functional characteristics of a chloride channel. J. Biol. Chem. *269*, 3339–3347.

Lavazec, C., Sanyal, S., and Templeton, T.J. (2007). Expression switching in the stevor and Pfmc-2TM superfamilies in *Plasmodium falciparum*. Mol. Microbiol. *64*, 1621–1634.

Ling, I.T., Florens, L., Dluzewski, A.R., Kaneko, O., Grainger, M., Yim Lim, B.Y., Tsuboi, T., Hopkins, J.M., Johnson, J.R., Torii, M., et al. (2004). The *Plasmodium falciparum* clag9 gene encodes a rhoptry protein that is transferred to the host erythrocyte upon invasion. Mol. Microbiol. *52*, 107–118.

Lisk, G., and Desai, S.A. (2005). The plasmodial surface anion channel is functionally conserved in divergent malaria parasites. Eukaryot. Cell *4*, 2153–2159.

Lisk, G., Pain, M., Gluzman, I.Y., Kambhampati, S., Furuya, T., Su, X.Z., Fay, M.P., Goldberg, D.E., and Desai, S.A. (2008). Changes in the plasmodial surface anion channel reduce leupeptin uptake and can confer drug resistance in *Plasmodium falciparum*-infected erythrocytes. Antimicrob. Agents Chemother. *52*, 2346–2354.

Marti, M., Good, R.T., Rug, M., Knuepfer, E., and Cowman, A.F. (2004). Targeting malaria virulence and remodeling proteins to the host erythrocyte. Science *306*, 1930–1933.

Pillai, A.D., Pain, M., Solomon, T., Bokhari, A.A., and Desai, S.A. (2010). A cell-based high-throughput screen validates the plasmodial surface anion channel as an antimalarial target. Mol. Pharmacol. *77*, 724–733.

Richard, D., MacRaild, C.A., Riglar, D.T., Chan, J.A., Foley, M., Baum, J., Ralph, S.A., Norton, R.S., and Cowman, A.F. (2010). Interaction between *Plasmodium falciparum* apical membrane antigen 1 and the rhoptry neck protein complex defines a key step in the erythrocyte invasion process of malaria parasites. J. Biol. Chem. *285*, 14815–14822.

Rungruang, T., Kaneko, O., Murakami, Y., Tsuboi, T., Hamamoto, H., Akimitsu, N., Sekimizu, K., Kinoshita, T., and Torii, M. (2005). Erythrocyte surface glycosylphosphatidyl inositol anchored receptor for the malaria parasite. Mol. Biochem. Parasitol. *140*, 13–21.

Russo, I., Babbitt, S., Muralidharan, V., Butler, T., Oksman, A., and Goldberg, D.E. (2010). Plasmepsin V licenses Plasmodium proteins for export into the host erythrocyte. Nature *463*, 632–636.

Saliba, K.J., Horner, H.A., and Kirk, K. (1998). Transport and metabolism of the essential vitamin pantothenic acid in human erythrocytes infected with the malaria parasite *Plasmodium falciparum*. J. Biol. Chem. *273*, 10190–10195.

Scherf, A., Lopez-Rubio, J.J., and Riviere, L. (2008). Antigenic variation in *Plasmodium falciparum*. Annu. Rev. Microbiol. *62*, 445–470.

Schmidt, J.A., Udeinya, I.J., Leech, J.H., Hay, R.J., Aikawa, M., Barnwell, J., Green, I., and Miller, L.H. (1982). *Plasmodium falciparum* malaria. An amelanotic melanoma cell line bears receptors for the knob ligand on infected erythrocytes. J. Clin. Invest. *70*, 379–386.

Spielmann, T., and Gilberger, T.W. (2010). Protein export in malaria parasites: do multiple export motifs add up to multiple export pathways? Trends Parasitol. *26*, 6–10.

Staines, H.M., Rae, C., and Kirk, K. (2000). Increased permeability of the malaria-infected erythrocyte to organic cations. Biochim. Biophys. Acta *1463*, 88–98.

Staines, H.M., Alkhalil, A., Allen, R.J., De Jonge, H.R., Derbyshire, E., Egée, S., Ginsburg, H., Hill, D.A., Huber, S.M., Kirk, K., et al. (2007). Electrophysiological studies of malaria parasite-infected erythrocytes: current status. Int. J. Parasitol. *37*, 475–482.

Trenholme, K.R., Gardiner, D.L., Holt, D.C., Thomas, E.A., Cowman, A.F., and Kemp, D.J. (2000). *clag9*: A cytoadherence gene in *Plasmodium falciparum* essential for binding of parasitized erythrocytes to CD36. Proc. Natl. Acad. Sci. USA *97*, 4029–4033.

Upston, J.M., and Gero, A.M. (1995). Parasite-induced permeation of nucleosides in *Plasmodium falciparum* malaria. Biochim. Biophys. Acta *1236*, 249–258.

Verloo, P., Kocken, C.H., Van der Wel, A., Tilly, B.C., Hogema, B.M., Sinaasappel, M., Thomas, A.W., and De Jonge, H.R. (2004). *Plasmodium falciparum*-activated chloride channels are defective in erythrocytes from cystic fibrosis patients. J. Biol. Chem. *279*, 10316–10322.

Vincensini, L., Fall, G., Berry, L., Blisnick, T., and Braun Breton, C. (2008). The RhopH complex is transferred to the host cell cytoplasm following red blood cell invasion by *Plasmodium falciparum*. Mol. Biochem. Parasitol. *160*, 81–89.

Wagner, M.A., Andemariam, B., and Desai, S.A. (2003). A two-compartment model of osmotic lysis in *Plasmodium falciparum*-infected erythrocytes. Biophys. J. *84*, 116–123.

Wellems, T.E., Oduola, A.M.J., Fenton, B., Desjardins, R., Panton, L.J., and do Rosario, V.E. (1988). Chromosome size variation occurs in cloned *Plasmodium falciparum* on *in vitro* cultivation. Rev. Brasil. Genet. *11*, 813–825.

Wellems, T.E., Panton, L.J., Gluzman, I.Y., do Rosario, V.E., Gwadz, R.W., Walker-Jonah, A., and Krogstad, D.J. (1990). Chloroquine resistance not linked to mdr-like genes in a *Plasmodium falciparum* cross. Nature *345*, 253–255.

Note Added in Proof

Comeaux et al. (2011) recently reported a recombinant *P. falciparum* line engineered to silence both *clag3* genes and observed significant growth inhibition relative to wild-type parasites. Their findings support an important role of the nutrient channel described here.

Comeaux, C.A., Coleman, B.I., Bei, A.K., Whitehurst, N., and Duraisingh, M.T. (2011). Functional analysis of epigenetic regulation of tandem *RhopH1/clag* genes reveals a role in *Plasmodium falciparum* growth. Mol. Microbiol. 80, 378–390.